

Experimental Evaluation of the Oxygen Microwave Absorption as a Possible Atomic Frequency Standard

JOHN M. RICHARDSON

National Bureau of Standards, Boulder Laboratories, Boulder, Colorado

(Received September 3, 1957)

A microwave absorption line of O_2 near 60 000 Mc has been experimentally investigated as a possible atomic frequency standard of high precision. Theoretical design, actual design, and results for an oxygen microwave spectrometer for use either in observing the line frequency or as a discriminator in a frequency control loop synchronizing an oscillator are described. Essential characteristics are the rate of change of spectrometer output signal with frequency and the output noise level. General expressions for these quantities for a wide range of experimental arrangements are obtained, and may be used to predict the attainable frequency precision. Characteristics in complete agreement with the theoretical values, capable of precision to less than 1 part in 10^9 , were experimentally observed with relatively crude apparatus. These characteristics involved line widths of around 560 kc and signal/noise ratios of 83 db. Improvement by a few orders of magnitude can be confidently expected by engineering refinements. An additional result was close confirmation of the theoretical absolute intensity of the $N_+ = 7$ line and a precision measurement of its frequency as $(60\,434.70 \pm 0.05)$ Mc.

INTRODUCTION

ONE of the resolved magnetic dipole transitions of O_2 arising from spin-rotation interaction lying near 60 000 Mc was suggested by Townes¹ and Lyons² as an atomic frequency standard possibly suitable for comparing or synchronizing an oscillator. Information available at that time indicated that an oxygen absorption spectrometer might surpass an ammonia absorption spectrometer principally because of the smaller dipole moment of O_2 . A quantitative experimental evaluation of an oxygen frequency standard would be helpful in comparing various devices including the subsequently developed cesium beam resonator and the ammonia maser. Thus the objective of the present investigation was to obtain experimentally for the oxygen line the highest signal/noise ratio in combination with the narrowest width possible, to extrapolate to expected results if any existing experimental limitations were to be overcome, and to use this information to estimate possible performance of an oxygen-controlled standard.

Rather extensive theoretical and experimental studies of oxygen exist on which to base the design of such an oxygen spectrometer. Beringer (1946)³ observed the absorption at atmospheric pressure; Van Vleck (1947)⁴ set down the basic theory; Burkhalter *et al.* (1950)⁵ observed the resolved spectrum at low pressure; Anderson *et al.* (1952)⁶ measured individual line width parameters, essentially confirmed by Artman and Gordon (1954)⁷; Hill and Gordy (1954)⁸ observed the temperature dependence of the line breadth parameter;

and Mizushima and Hill (1954)⁹ refined the theory. In addition, several other confirming and extending investigations have been made which are listed for reference.¹⁰

I. THEORETICAL DESIGN

In considering an oscillator of frequency control characteristic K (cycles/volt) controlled by a frequency sensitive element (a discriminator) as in Fig. 1, the two essential factors governing the residual frequency deviations resulting from noise $\delta\nu_n$, are the slope of the discriminator output characteristic D , (volts/cycle) and the open-loop noise voltage at the discriminator output V_{n0} , related by

$$\delta\nu_n = KAV_{n0}/(1+KAD) \approx V_{n0}/D \quad (1)$$

for large amplifier gain, A . We may define a stabiliza-

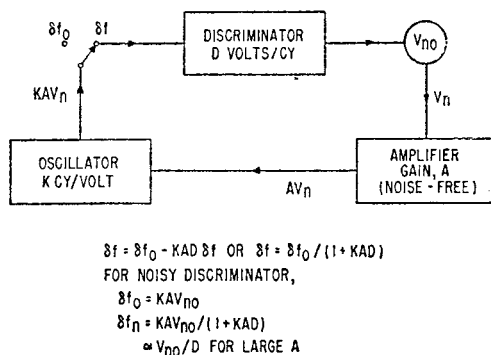


FIG. 1. Oscillator controlled by frequency discriminator and feedback loop. Subscript 0 refers to conditions when the loop is open.

¹ C. H. Townes, J. Appl. Phys. 22, 1365 (1951). Some corrections noted by C. R. S. Ince, J. Appl. Phys. 23, 1408 (1952).
² Harold Lyons, Ann. N. Y. Acad. Sci. 55, 831 (1952).
³ Robert Beringer, Phys. Rev. 70, 53 (1946).
⁴ J. H. Van Vleck, Phys. Rev. 71, 413 (1947).
⁵ Burkhalter, Anderson, Smith, and Gordy, Phys. Rev. 79, 651 (1950).
⁶ Anderson, Smith, and Gordy, Phys. Rev. 87, 561 (1952).
⁷ J. O. Artman and J. P. Gordon, Phys. Rev. 96, 1237 (1954).
⁸ R. M. Hill and W. Gordy, Phys. Rev. 93, 1019 (1954).

⁹ M. Mizushima and R. M. Hill, Phys. Rev. 93, 745 (1954).
¹⁰ Strandberg, Meng, and Ingersoll, Phys. Rev. 75, 1524 (1949); B. V. Gokhale and M. W. P. Strandberg, Phys. Rev. 84, 844 (1951); S. L. Miller and C. H. Townes, Phys. Rev. 90, 537 (1953); M. Tinkham and M. W. P. Strandberg, Phys. Rev. 97, 937 (1955); 99, 537 (1955).

tion ratio S at the frequency ν , such that,

$$S^{-1} \equiv \delta\nu_n/\nu = V_{n0}/\nu D. \quad (2)$$

This quantity also expresses the relative precision to which ν can be observed in the presence of noise, even if the feedback loop is not closed. The discriminator may be considered to consist of the microwave absorption cell and the associated rf detector, which together convert frequency information into a voltage V , which may be used to provide the corrective feedback. The voltage V , is the usual resonance type of response (Fig. 6) and is a function of the gas absorption coefficient γ , which is in turn a sharp function of ν . A typical discriminator response curve may be provided from V simply by taking as a function of frequency the difference in response for points separated in frequency by a constant. This arrangement has the practical benefits of symmetry, balance, and null detection. The frequency stability of the discriminator response itself is at present assumed to be indefinitely great by virtue of its derivation from a spectral line. The validity of this assumption will later be qualitatively discussed. Design of an oxygen atomic frequency standard will thus center about achieving the greatest value of D and the least value of V_{n0} as they depend on gas, absorption line, pressure, temperature, power level, detector characteristics, and so forth.

If the line may be considered symmetrical, then at the crossing of the discriminator characteristic,

$$D = 2dV/d\nu = 2(dV/d\gamma)(d\gamma/d\nu), \quad (3)$$

where $dV/d\gamma$ may be evaluated at any desired frequency by proper choice of the above frequency separation. The γ used here is the absorption coefficient appropriate to the gas in the wave guide and is related to the intrinsic absorption of the medium, γ_i by

$$\gamma = (\lambda_g/\lambda)\gamma_i, \quad (4)$$

where λ is the free space wavelength and λ_g is the guide wavelength.

It is now convenient to express Eq. (2) involving V and V_{n0} in terms of the available powers involved, which is easily done by noting that the actual voltage, V , across some load resistance is proportional to the square root of the available power from the internal impedance of the discriminator, and by noting that the actual noise voltage across some (noiseless) load resistance is also proportional, with the same constant of proportionality, to the square root of the equivalent available noise power from the discriminator internal impedance. Thus we substitute in Eqs. (2) and (3),

$$\begin{aligned} V &\propto (GP_s)^{\frac{1}{2}} \\ V_{n0} &\propto (FGkT_0B)^{\frac{1}{2}}, \end{aligned} \quad (5)$$

where P_s is the rf signal power defined below; G is the available power gain of the detector, its functional form depending on whether a linear or square law

detector is used; F is the overall noise figure of the detector and amplifier combination; k is Boltzmann's constant; T_0 is the reference temperature to which the noise figure is referred; and B is the band width.

In accordance with common usage we take

$$FGkT_0B = [G(s-1) + F_A + t - 1]kT_0B, \quad (6)$$

for a source at noise temperature s , detector at noise temperature t , and amplifier of noise factor F_A following the detector.

In the case of a square wave modulated spectrometer of length l and input power P_0 , in which the total absorption rate is alternately varied from the waveguide power attenuation rate α to $\alpha + \gamma$, the total power introduced as fundamental frequency sidebands is

$$P_s = (2/\pi^2)P_0e^{-\alpha l}(1 - e^{-\gamma l/2})^2. \quad (7)$$

From the approximate shape of a well-resolved microwave spectral line of peak absorption γ_0 , center frequency ν_0 , and "half-half width" $\Delta\nu$,

$$\gamma = \frac{(\Delta\nu)^2}{(\nu - \nu_0)^2 + (\Delta\nu)^2} \gamma_0 = \frac{1}{1 + a^2} \gamma_0, \quad (8)$$

where

$$a = (\nu - \nu_0)/\Delta\nu. \quad (9)$$

Carrying out the differentiations indicated in Eq. (3) and remembering that in general G may be a function of γ , we have finally,

$$\begin{aligned} \frac{\delta\nu_n}{\nu_0} &= \frac{\sqrt{2}\pi}{2\{1 + [(e^{\gamma l/2} - 1)/G](dG/d\gamma l)\}} \left(\frac{FkT_0B}{P_0e^{-(\alpha+\gamma)l}} \right)^{\frac{1}{2}} \\ &\quad \times \frac{(1+a^2)^2 \Delta\nu}{2a} \frac{1}{\nu_0 \gamma_0 l}. \end{aligned} \quad (10)$$

There is still some interdependence among the variables: in particular, G for a square law detector depends on the power level at the detector, which in turn involves P_0 , α , γ , and l . Similarly F , through G , t , and s depends on the same quantities. Also $\Delta\nu$ and γ_0 depend on the power level in the cell because of power saturation. And γ is a function of a and γ_0 , while a depends on ν and $\Delta\nu$. There is, furthermore, additional dependence of the explicit variables on other experimental variables such as pressure, temperature, cell transverse dimensions, and rotational quantum number, which specifies the particular transition chosen. Thus, Eq. (10) may be viewed as a composite function of the m explicit variables (x_1, \dots, x_m) subject to k constraints of the form

$$\phi_i(x_1, \dots, x_m) = 0, \quad n > m; \quad i = 1, 2, \dots, k. \quad (11)$$

Equation (10) could in principle be exactly minimized by the method of Lagrange's multipliers, but for the initial design, an approximate minimization carried out with less effort will serve as well.

The further dependence of the quantities in Eq. (10) on still other experimental variables is collected below for reference.

The intrinsic absorption at the resonant frequency and for zero power, γ_{i0} , as limited by pressure broadening, the only case considered here, is given as a function of rotational quantum number N by either

$$\gamma_{i0+}(N) = \left(\frac{8\pi\mu_0}{3k}\right)^2 \left(\frac{Bh}{c}\right) \left(\frac{L_0 T_0}{p_0}\right) \frac{N(2N+3)}{(N+1)} \times \frac{1}{T^3} \frac{\nu_+^2(N)}{(\Delta\nu/p)} e^{-BhN(N+1)/kT}, \quad (12)$$

$$\text{or,} \quad \gamma_{i0-}(N) = \left(\frac{8\pi\mu_0}{3k}\right)^2 \left(\frac{Bh}{c}\right) \left(\frac{L_0 T_0}{p_0}\right) \frac{(N+1)(2N-1)}{N} \times \frac{1}{T^3} \frac{\nu_-^2(N)}{(\Delta\nu/p)} e^{-BhN(N+1)/kT}, \quad (13)$$

where + or - indicates the transitions $J=N+1 \rightarrow J=N$ and $J=N-1 \rightarrow J=N$, respectively. In these expressions μ_0 is the Bohr magneton; k is Boltzmann's constant; h is Planck's constant; c is the speed of light; L_0 is Loschmidt's number, T_0 and p_0 are here standard gas temperature and pressure; B is a molecular constant such that $B/c=1.44 \text{ cm}^{-1}$; T is the absolute temperature, $\nu_+(N)$ or $\nu_-(N)$ the resonant frequency of the + or - transition for particular N , $(\Delta\nu/p)$ the line width parameter for a given line for zero power such that for pressure broadened lines the actual line width at the pressure p is $\Delta\nu$. It has been found experimentally⁹ that $(\Delta\nu/p)$ varies approximately as $T^{-0.9}$. The absorption and the line width actually depend on the intensity of the radiation because of power saturation. For non-zero power γ_{i0} and $\Delta\nu$ should be everywhere replaced by

$$\gamma_{i0} \rightarrow \gamma_{i0} [1 + 4\pi |\mu|^2 P_0 / 3ch^2 A (\Delta\nu)^2]^{-1} \quad (14)$$

and

$$\Delta\nu \rightarrow \Delta\nu [1 + 4\pi |\mu|^2 P_0 / 3ch^2 A (\Delta\nu)^2]^{\frac{1}{2}}, \quad (15)$$

if we take P_0 as the approximate power level by which to describe saturation. Here μ is the dipole moment of the transition as given by Van Vleck,⁴ and A is the cross-sectional area of the wave guide absorption cell.

For a square law detector it is easy to show by direct comparison of P_s and the power available from the detected voltage, that

$$G = (k_0^2/r) H P_0 e^{-\alpha l}, \quad (16)$$

where k_0 is the open-circuit peak voltage sensitivity of the detector to power changes at the fundamental modulation frequency, in potential per unit rf power, r is the detector internal impedance, $H = [1 - (1/2) \times (1 - e^{-\gamma l/2})]^2 = [(1/2)(1 + e^{-\gamma l/2})]^2$, a factor correcting for the variation in conversion efficiency between the full power portion of the modulation cycle and the absorbing portion when the rf power at the detector is

reduced by the fraction $e^{-\gamma l}$ of its full value. For a linear detector, G may be taken as constant, independent of P_0 , α , γ , and l . Also, for a linear detector, $dG/d\gamma l = 0$, and even for a square law detector it is always less than unity, tending to zero as γ tends to zero.

For a linear detector consisting of a crystal mixer, t may be taken as constant independent of other quantities in Eq. (10) for given operating conditions of local oscillator excitation and noise. For a crystal video detector t depends strongly on incident rf power and also on modulation frequency as summarized by Strandberg *et al.*¹¹ For a bolometer, t is a constant for given operating conditions of bias. The noise caused by the source, skT is proportional to the level of source power, and hence depends on P_0 , α , γ , and l . There may furthermore be a significant dependence on frequency separation from the carrier frequency.

Finally, we have the dependence of α on the cross-sectional dimensions of the wave guide, and on the temperature, as obtainable from handbooks.

The design of the frequency standard will consist of minimizing Eq. (10) with respect to all independent variables. This process will yield slightly different results depending on what assumptions and approximations are made, but it should give a good approximate first design, which can itself be evaluated more exactly by Eq. (10) when completed.

II. ACTUAL DESIGN

The general features of Eq. (10) are worth noting. There will be an optimum length both for a linear detector and a square law detector, dependent on α and γ . The effect of the temperature dependence of α will be slowly varying since α is inversely proportional to the square root of the conductivity, which in turn varies nearly linearly with temperature. Thus, although it will be helpful to lower α by operating at a low temperature, the main temperature dependence occurs in $\Delta\nu/\gamma_0$. For low N , the temperature variation of the exponential in γ_0 is not severe between 40°K and 300°K, so that the main variation is about as $T^{-2}T^0 = T$. It is thus desirable to lower the operating temperature within limits, and initial operation at liquid nitrogen temperature (76°K at Boulder) appeared a good practical choice.

Choice of N is best made by computing $\gamma_{i0}(N)$ for the + and - transitions at the design temperature, and picking the strongest line, since $\Delta\nu$ is essentially independent of N for this purpose.

Choice of wave-guide size is motivated by the desire to use large wave guide to reduce both α and power density P_0/A and the desire to use small wave guide to avoid difficulties of multi-mode transmission including consequent uncertainty about the form of the inter-

¹¹ Strandberg, Johnson, and Eshbach, *Rev. Sci. Instr.* **25**, 776 (1954).

TABLE I. Reported variation of line width parameter and peak absorption with rotational quantum number and temperature.^a

A.	Line width parameter, $\Delta\nu/p$ (in units of Mc/mmHg)					
	300°K		76°K		45°K	
N	-	+	-	+	-	+
1	(2.06) ^b	2.20	(7.09) ^c	7.57	(11.4) ^c	12.1
3	1.94 ^b	2.23	6.23	7.16	9.73	11.2
5	1.99	1.96	6.39	6.74	9.98	10.8
7	1.82	1.92	5.77	6.17	8.96	9.63
9	2.00	1.93	5.69	5.48	8.46	8.16
11	1.97	1.94 ^b				
13	1.86	1.94 ^b				

B.	Peak absorption, γ_{10} (in units of 10^{-6} cm^{-1})					
	300°K		76°K		45°K	
N	-	+	-	+	-	+
1	(14.6) ^c	3.83	(250) ^c	65.8	(722) ^c	191
3	13.3	10.3	200	154	493	379
5	17.3	17.2	168	156	316	286
7	21.0	20.8	130	127	141	137
9	18.6	21.2	64	74	39	44
11	16.7	19.6				
13	14.4	16.6				

C.	Ratio of peak absorption to line width parameter, $\gamma_{10}/(\Delta\nu/p)$ (in units of $10^6 \text{ cm}^{-1} - \text{mmHg/Mc}$)					
	300°K		76°K		45°K	
N	-	+	-	+	-	+
1	(7.09) ^c	1.75	(35.3) ^c	8.69	(63.3) ^c	15.8
3	6.86	4.62	32.1	21.5	50.7	33.8
5	8.69	8.78	26.3	23.1	31.7	26.5
7	11.5	10.8	22.5	20.6	15.7	14.2
9	9.3	11.0	11.3	13.5	4.6	5.4
11	8.5	10.1				
13	7.7	8.6				

^a Calculations made from Eqs. (12) and (13) using values of line width and its temperature dependence reported in references 7 and 8.

^b Theoretical value; no observation.

^c 119 kMc line.

action of the radiation with the molecule. Large wave guide also insures that wall-collision broadening is small.

As long as we are below power saturation we want P_0 large and $\Delta\nu$ (which is proportional to p) small. However, if saturation is taken into account, Eq. (10) has the following dependence on pressure and power neglecting $dG/d\gamma l$, using Eqs. (14) and (15), introducing the abbreviation $x^2 = P_0/p^2$, the obvious abbreviations b and C , and recalling that $(\Delta\nu/p)$ and γ_0 , quantities defined for zero power, are independent of p and P_0 ,

$$\frac{\delta\nu_n}{\nu_0} \propto x^{-1}(1+Cx^2)^{\frac{1}{2}} \exp[b/2(1+Cx^2)]. \quad (17)$$

Thus Eq. (17) is a function of $P_0^{\frac{1}{2}}/p$ only and has a minimum for

$$2Cx^4 + (1-b)Cx^2 - 1 = 0. \quad (18)$$

If $b \ll 1$ (small $\gamma_0 l$) Eq. (19) yields the more familiar root,

$$2CP_0/p^2 = 1. \quad (19)$$

These relations have the remarkable effect of making the frequency precision independent of line width (or pressure) for given T . If G depends on P_0 an optimum pressure and power will be found.

The greatest effect of a will be produced by the factor $(1+a^2)^2/2a$, which has minimum value at $a = \pm 1/\sqrt{3}$. Even if the dependence of γ on a is taken into account, no result different by a large factor will occur.

Closer evaluation of the benefits of lowering the temperature may now be made. At optimum power determined by Eq. (19), if free choice of N is allowed, we see an indicated 5-fold improvement in $\gamma_0/(\Delta\nu/p)$ in Table I. C by going from 300°K to 45°K, about the lowest temperature at which there is sufficient vapor pressure to allow pressure broadening to predominate over Doppler broadening. For less than optimum power the governing factor is γ_0 and we see a possible 25-fold improvement for given $\Delta\nu$ from inspecting γ_0 in Table I. B. At 76°K, a convenient temperature from the experimental standpoint, the + or - transitions of $N=3, 5, \text{ or } 7$ work fairly well for either low power or optimum power. The $N_+=7$ line at 60.435 kMc was experimentally convenient as to frequency, and was chosen.

Wave guide size RG-96/U, 0.140 in. \times 0.280 in., was chosen as fairly well satisfying the criteria mentioned above. For this wave-guide size in coin silver ($\sigma = 3.33 \times 10^7 \text{ mho-m}^{-1}$ at room temperature) at 60.435 kMc,

$$\alpha = 1510 \times 10^{-6} \text{ cm}^{-1} \text{ at } 300^\circ\text{K},$$

and

$$\alpha = 710 \times 10^{-6} \text{ cm}^{-1} \text{ at } 76^\circ\text{K}.$$

From Table I, for the $N_+=7$ line,

$$\gamma_{10} = 21 \times 10^{-6} \text{ cm}^{-1} \text{ at } 300^\circ\text{K},$$

and

$$\gamma_{10} = 127 \times 10^{-6} \text{ cm}^{-1} \text{ at } 76^\circ\text{K}.$$

Values for the intrinsic absorption are quoted here since the correction factor to wave-guide absorption, λ_a/λ , only differs from unity by 7% in this case.

Equation (10) may now be maximized with respect to l . It seems wise to eliminate the dependence of F on l by adopting a scheme to balance out any source noise, and by using a detector with l independent of l . At $a = 1/\sqrt{3}$, $\gamma = 3\gamma_0/4$, and for a linear detector

$$l_{\text{opt}} = 2/(\alpha + \gamma), \quad (20)$$

which yields 2390 cm at 76°K.

The optimum length for a square law detector would be about half this. Such a cell was clearly impractical at first so the length was chosen to be 746 cm (at 76°K) or about 25 feet, as long as was considered convenient.

The relationship of Eq. (18) gives numerically, for a linear detector, under these conditions,

$$(P_0)_{\text{opt}}/p^2 \approx 3w - \text{mmHg}^{-2} \text{ at } 300^\circ\text{K},$$

and

$$(P_0)_{\text{opt}}/p^2 \approx 30w - \text{mmHg}^{-2} \text{ at } 76^\circ\text{K}.$$

Thus even at 0.02 mm pressure it is just beyond the present state of the millimeter wave art to provide the optimum 12 mw required at 76°K. Nor is it likely the

present linear or square law detectors will operate at these high levels. It appears that the evaluation will have to be carried out at less than optimum power.

The square wave modulation of intensity assumed above was achieved by applying a square wave magnetic field parallel to the cell axis. This has the effect of resolving the $3(2J'+1)$ Zeeman components, where J' is the total angular momentum quantum number of the lower state. One unshifted π component remains at the unresolved line frequency, and this is very weak because of both the resolution of the line into the other Zeeman components and the fact that this one is excited only by the longitudinal component of the microwave magnetic field, which in turn is only part of the whole field. Thus when the Zeeman field is on, the gas absorption may be considered approximately zero, and when the Zeeman field is off it has its normal value given by Eqs. (12) and (13). The required magnitude of the field is not critical just so it is above the value necessary to remove all the Zeeman components from the neighborhood of the unshifted frequency. Typically this is perhaps 90 gauss, and may be checked experimentally by increasing the field until no further increase in signal strength is observed.

Limitations on the modulation frequency arise from several sources—the near-carrier noise spectrum of the source; the excess noise spectrum of the detector, the frequency response of the solenoid, which is actually a lossy, slow wave transmission line; the shielding effect of the wave guide; and the detector frequency response. The source spectrum limitation may be avoided by source noise balancing. The excess noise of a crystal rectifier may be avoided by using a high modulation frequency, superheterodyne detector, or a bolometer, which is nearly excess noise free. The solenoid frequency response limitation is a serious one, restricting us to frequencies well below that for which the wavelength of the solenoid is $\lambda/4$. For the two-layer solenoid used this critical frequency was about 10 kc. The wave-guide shielding became noticeable at about 1 kc, so that the highest harmonic which is desired to contribute to the modulating wave form should not be above this, unless the shielding is alleviated by splitting and insulating the wave guide lengthwise. From these considerations it is seen that source noise balancing in combination with an excess noise-free detector is indicated so as to place no lower limit on the modulation frequency. This choice has the additional benefit of not prejudicing the use of a bolometer, which has good response only at low frequencies.

Decision between superheterodyne and square law detector will be made largely on the basis of a comparison of F for the two cases. In either type of detector it will be advisable to use balancing difference amplifiers as shown in Fig. 2, to eliminate the term $(s-1)$ in Eq. (6) for the noise figure. The noise figure, F_A , of this amplifier may be shown to be

$$F_A = F_{A0} + t_2 - 1, \quad (21)$$

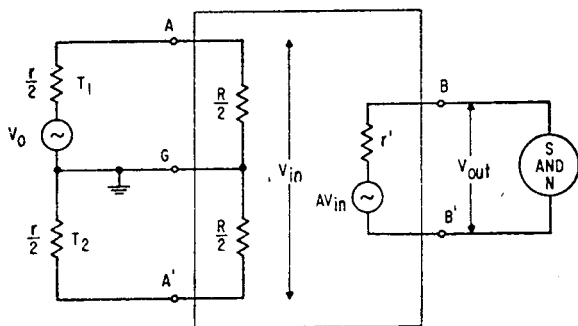


FIG. 2. Difference amplifier showing impedance, signal, and noise relations. Common phase source noise applied to terminals AG and $A'G$; gas signal V_0 applied to AG only.

where F_{A0} is its noise figure when $t_2 \equiv T_2/T_0 = 1$. Furthermore, when the amplifier terminals AA' must be fed by the bucking detectors as shown, the available power gain is just one-half the value it would be if the terminals AA' could be fed by the signal detector only, but transformed up to the same impedance level as the two series bucking detectors. This means that F_{A0} is twice that which could be attained by a single-ended arrangement. The balanced arrangement then suffers by increased amplifier noise figure and the addition of $t_2 - 1$ for the balancing detector.

For a superheterodyne receiver with crystal mixer the limiting theoretical value of G is unity, but in a practical case at 60 kMc it is more likely to be about $1/10$. In Eq. (21) we may put $F_{A0} = 2.8$ for a good difference I.F. amplifier, $t_1 - 1 = t_2 - 1 = 3$ to obtain

$$F_{lin} = 88.$$

For the square law detector if we take $H \approx 1$, $P_0 e^{-\alpha l} \approx 10^{-2} w$, $k_0 = (10 \Omega/mw) \times (3 \text{ ma}) = 30 \text{ v/w}$, and $r = 200 \Omega$ as typical of a sensitive bolometer, $F_{A0} = 4$, $t_1 - 1 = t_2 - 1 = 6$, we have

$$F_{sq} = 3500,$$

and the ratio of $F^{\frac{1}{2}}$ for the two types of detector is 6 in favor of the superheterodyne, which is not an overwhelming advantage.

For the square law detector, G varies in proportion to the power at the detector, $P_0 e^{-\alpha l}$, so that for low power the square law detector is at a definite disadvantage. For power greater than a few milliwatts the proportionality will break down, so that the square law detector ceases to gain on the linear detector. Since the performance of the two types of detector is not vastly different for the milliwatt power range, and since the bolometer is considerably simpler than a millimeter wave superheterodyne receiver, it was chosen. It has already been indicated that the excess noise of a crystal rectifier at milliwatt powers and low frequencies made its use undesirable. In addition, the crystal rectifier usually deviates from square law response at around $10 \mu w$, so that these facts confirmed the choice of the bolometer as a detector. In fact, it was experimentally observed that the signal-

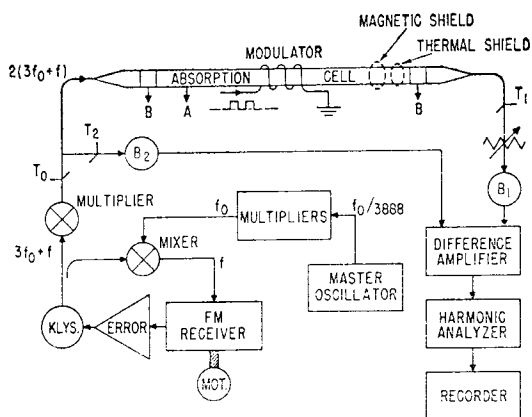


FIG. 3. Experimental arrangement of oxygen microwave spectrometer.

to-noise ratio was better with the bolometer than with the crystal under the actual operating conditions for just the reasons stated.

The apparatus resulting from the above design considerations is shown in Fig. 3. The source frequency is derived for convenience from a QK-290 reflex klystron which is stabilized with respect to a multiple of the master oscillator by the subsidiary afc loop shown. For actual frequency standard operation the klystron must be locked absolutely to the stable frequency, which in turn would be controlled by the loop of Fig. 1, but for the purpose of measuring discriminator slope and noise it was sufficient that the spectral width of the source be small compared with the line width. This requirement was satisfied with about 6 kc half width at 60 kMc for the apparatus shown, with respect to the master oscillator multiple. The master oscillator was stable to about 1 part in 10^7 as measured by the standard deviation of a group of counts within the space of 1 hour so that the absolute spectral width may have been as much as $6\sqrt{2}$ kc at 60 kMc. The long term drift of the master oscillator was 4×10^{-9} per day. Frequency measurements were calibrated directly against the national standard of frequency.

The source frequency could be tuned by tuning the FM receiver in the stabilizing loop. The mixed frequency f was around 59 Mc. The silicon diode doubler was of the type described by Richardson and Riley¹² and delivered up to 2 mw out for 80 mw in. The microwave power was split at the tee junction, and part was immediately detected in B_2 and part transmitted down the cell and detected in B_1 . T_0 and T_2 were set to effect such a power division that source modulation common to both paths was recovered equally, and cancelled in the difference amplifier. Rejection ratios of 60 to 100:1 could be obtained and maintained over the line width, and this was sufficient to make the contribution of $G(s-1)$ in Eq. (6) negligible compared to $F_A + t - 1$,

thus completely removing trouble from source noise. Short-term power stability was good enough to observe the lines with no distortion, but in terms of hours there was some power drift. The effects of this in an actual frequency standard would be avoided by the technique of simultaneously (or alternately) observing both slopes of the line.

The absorption cell itself was connected to vacuum system, A , instrumented for gas handling and pressure measurement. To avoid frosting of the inner window when the cell was cooled, evacuated guard sections, B , were added with the outer window at room temperature. The Zeeman modulation solenoid was concentric with the cell and consisted of a double layer of 0.057 in. \times 0.064 in. enameled rectangular wire so as to get the greatest volume of copper in the available space, thus allowing the greatest field for a given power dissipation. The coil could be switched from the modulator to a dc current source and potentiometer so that it could also be used as a resistance thermometer.¹³

The thermal shield was a double-walled evacuated brass jacket concentric with the cell. It served also as the container for liquid N_2 coolant, the latter being pumped lightly to avoid condensation of atmospheric oxygen and consequent warming. The magnetic shield was 0.030 in mu-metal, and was used to prevent line broadening by incipient splitting in the earth's field.

The difference amplifier drove the harmonic analyzer, which was used as a narrow band VTVM limiting the effective system band width to 8 cps. Its output, approximately proportional to rms signal or noise input, was further averaged and recorded. Adequate linear dynamic range from noise to peak signal was provided by calibrated attenuators in the detecting system. Care was taken that 60 cps pickup was negligible compared to all observations.

The modulator was an audio power amplifier driven by a square wave generator, feeding the modulation coil through a sufficiently high resistance to secure fairly good current wave form, and through a hard tube series diode to provide zero basing and unidirectional field. Figures 4 and 5 show observed signal

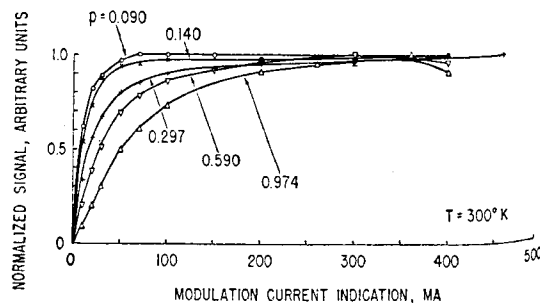


FIG. 4 Absorption signal vs modulation current showing variation with Zeeman field. $T = 300^\circ\text{K}$. Pressures in mmHg.

¹² J. M. Richardson and R. B. Riley, *Inst. Radio Engrs., Trans. Microwave Theory and Tech.* **MTT-5**, 131 (1957).

¹³ T. M. Dauphinee and H. Preston-Thomas, *Rev. Sci. Instr.* **25**, 884 (1954).

strengths as a function of modulation current at 30 cps for various pressures and temperatures. It is seen that full signal occurs early for narrow lines, and later for broad lines as expected. The operating current was set well into the region of full signal to insure that the line was being completely resolved and that a true intensity was being observed.

The sensitivity of the bolometers, k_0 , is proportional to bias current but also varies from type to type (cartridge or wafer) and from unit to unit of the same type for given bias. It could be conveniently measured by applying a square rf pulse of known average power, and observing the output voltage. In this way it was found that wafer bolometers were generally more sensitive (about $10\Omega/\text{mw}$) and more uniform (1.5-fold sensitivity range) than cartridge types (about $1\Omega/\text{mw}$ and 5-fold range). In addition it was found unwarranted to assume $l=1$ for a bolometer since very appreciable noise is produced by applying the bias current through the Wollaston wire contacts. Indeed $l \approx 1$ was observed to range from twenty to several hundreds at rated bias current. In general an improvement in the ratio of sensitivity to noise temperature could be obtained by derating the bias current, which usually caused the noise to fall faster than the sensitivity.

It is true that the arrangement of the difference amplifier and the balance bolometer, B_2 , acted to raise the noise figure, F_A , over that which could be attained with single ended operation alone. In fact, $F_A \approx 2$ for single ended operation and $F_A \approx 40$ for balanced operation caused mainly by the hot bolometer B_2 . Nevertheless the sacrifice was very worthwhile in achieving a net noise reduction by eliminating very severe source noise.

III. RESULTS

The observations consisted of recording the signal intensity as the source frequency was swept across the line, and of recording the noise level when the signal was absent by reason of the modulation being turned off. The signal recordings were made both at room temperature and at liquid nitrogen temperature, and at various pressures. Power level at the detector, $P_0 e^{-(\alpha+\gamma)l}$, was noted for each run so that results could

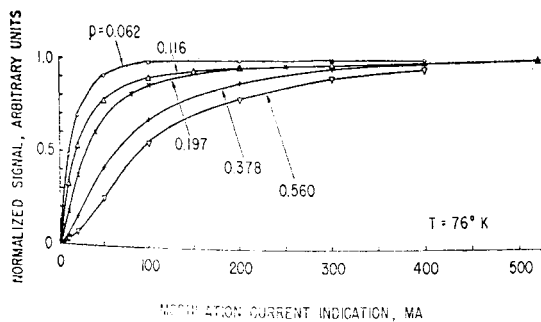


FIG. 5. Absorption signal vs modulation current showing variation with Zeeman field, $T=76^\circ\text{K}$. Pressures in mmHg.

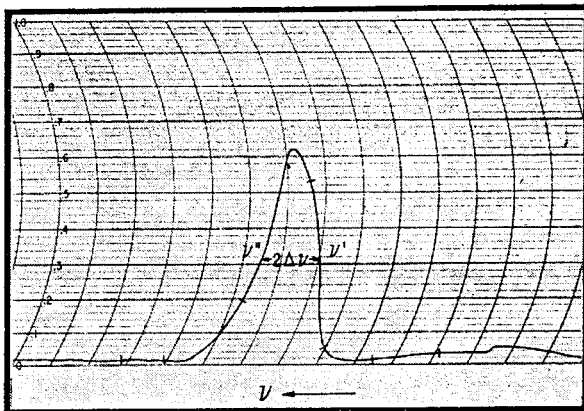


FIG. 6. A line recording. $T=75^\circ\text{K}$. $p=0.065$ mmHg. Power at detector = $120\ \mu\text{v}$. $\Delta\nu=330$ kc.

be reduced to a common power basis. An example of these observations is shown in Fig. 6.

Thus the observations provided immediately the quantity $V_{n0}/\nu_0 D$ necessary to evaluate the attainable precision of observation of ν or of an afc system based on a given condition of operation of the present apparatus. In addition, observations were also made of quantities entering into the right member of Eq. (10) so that the observed magnitude of $V_{n0}/\nu_0 D$ could be checked by Eq. (10). Having obtained satisfactory checks for the actual conditions of operation, extrapolation for improved operating conditions such as more power, narrower line, longer cell, etc., could be made with some confidence.

Of the observed quantities on the right in Eq. (10), γ_0 and $\Delta\nu$ may be separately and conveniently checked against their theoretical behavior, since the power level used was always well below incipient saturation. The absorption, γ_0 , is related to the observed rms signal voltage V by Eqs. (5) and (7), using Eq. (16) for the square law detector. Thus,

$$V = (\sqrt{2}/\pi) k P_0 e^{-\alpha l} (1 - e^{-\gamma l}), \quad (22)$$

in which k , the actual voltage sensitivity of the bolometer as connected, and l are known, and $P_0 e^{-(\alpha+\gamma)l}$ was measured. This may be numerically evaluated for γ by successive approximation of

$$\gamma = -\frac{1}{l} \ln_e \left[1 - \frac{V e^{-\gamma l}}{(\sqrt{2}/\pi) k P_0 \exp[-(\alpha+\gamma)l]} \right], \quad (23)$$

where an approximate value of γ may be used in the right member. Observed results, constituting one of the few observations on absolute intensities of O_2 , are presented in Table II. The method is reasonably insensitive to errors in bolometer power measurement since the same bolometer and bolometer bridge were used to measure both P_0 and the power for calibrating k in Eq. (23). The data at the 30 cps modulation frequency f_z , are considered much more reliable than at 90 cps, because of observed poor wave shape during the

TABLE II. Observations of absolute peak absorption intensity under various experimental conditions.

f_z (cps)	T (°K)	p (mmHg)	$10^6\gamma_{10}$ (calculated) (cm^{-1})	$10^6\gamma_{10}$ (observed) (cm^{-1})
30	298	0.276	20.7	17.0
		0.556		18.7
		0.974		19.7
	75	0.062	127	82.6
		0.116	127	92.9
		0.197	130	104
		0.378	127	115
	90	298	0.225	20.7
0.264			10.7	
0.34			11.8	
0.591			11.0	
1.44			9.5	
75		0.24	127	73.4
115		0.29	87.2	40.5
77		0.48	125	53.8

off cycle and consequent line broadening with reduction in peak intensity. The wave shape at 30 cps was free from this defect, and these data are very satisfactory for the present purpose. It is not possible to say whether the apparent small increase in γ_0 with p is real, since it could also be caused by the above instrumental imperfection in the off cycle wave shape. The technique is capable of further refinement to give better absolute intensities.

The situation with regard to the line width was less satisfactory in that the above instrumental imperfections of poor off cycle wave shape and insufficient available modulation at the higher pressures prevented the accurate measurement of actual line width over a wide range of pressure and temperature. It can be said, however, that in regions where these imperfections were not serious, fair agreement with the well established values^{6,7} was obtained, and the inverse temperature dependence⁸ was semiquantitatively confirmed. It can be seen that insufficient modulation, which will tend to occur at the higher pressures, will fail to resolve the Zeeman components completely during the on cycle and will give too narrow a line width. Similarly, failure to establish zero Zeeman field during all of the off cycle will broaden the line during the off cycle, and give too wide a line width, especially at the lower pressures. These effects are nonfundamental in nature, and may easily be eliminated by improved modulator design. At any rate, the expected line widths could be achieved within certain ranges of the experimental variables, and since there are strong theoretical reasons to support the present view of line width and its pressure variations, we may use the theory with confidence for extrapolation.

Separate measurements of $F_{A_0}=5$, $t_2-1=6$, $t_1-1=8$ predicted the equivalent noise in the detector load as $19kT_0B$, agreeing exactly with the directly observed value of $19kT_0B$. As mentioned above, a condition of balance could be found so that addition of source

TABLE III. Comparison of S^{-1} directly observed as $V_{n0}/\nu_0 D$ and calculated as $\delta\nu_n/\nu_0$ from observed quantities on the rhs of Eq. (10) for various experimental conditions. Band width = 8 cps.

T (°K)	p (mmHg)	Power at detector (μw)	$V_{n0}/\nu_0 D$	$\delta\nu_n/\nu_0$
76	0.114	130	6.4×10^{-10}	6.0×10^{-10}
75	0.116	130	5.7	6.2
72	0.197	170	4.6	5.8
298	0.270	54	130	130
	0.34	70	75	75
	0.556	86	75	90

power without Zeeman modulation caused essentially no change in the output noise level.

Selection of several experimental runs having the most favorable combination of the quantities in Eq. (10) gave the comparison of Table III between S^{-1} directly measured from the records as $V_{n0}/\nu_0 D$, and as $\delta\nu_n/\nu_0$ calculated from observations on the rhs of Eq. (10) for the 8-cps band width used. For the best run, the line width was 560 kc and the signal/noise ratio at peak absorption was 83 db. It is seen that agreement is good to within a few percent, showing that the expectations from oxygen are completely realizable by experiment. It is thus valid to estimate what value of $\delta\nu_n/\nu$ may be expected by further refinement of apparatus and experimental conditions. Those conditions which may reasonably be attained by the present state of the art are tabulated in Table IV along with the value of $\delta\nu_n/\nu$ they produce, so that a feeling may be obtained for the magnitudes involved. Also included is a calculation based on the foregoing principles for near-optimum conditions, regardless of present expectations of attaining them. The figure for frequency precision may be compared with that of $\delta\nu_n/\nu=5 \times 10^{-15}$ predicted by Townes¹ for oxygen.

The average of the two half-power frequencies was observed to 0.01 Mc and this figure was taken as ν_0 . To this precision, an apparent frequency shift caused by asymmetry in the Van Vleck-Weisskopf (VV-W) line shape is negligible at the line widths in use. The scatter in all (some 43) observations of ν_0 was confined to a spread of 0.5 Mc, with a standard deviation of 0.1 Mc, for a range of pressures from 0.012 mmHg to 1.44 mmHg and temperatures from 72°K to 298°K. There is no clear evidence of a shift in ν_0 with pressure or temperature to this precision within these ranges. Our best evaluation of the resonant frequency of the $N_+ = 7$ line is

$$\nu_0 = (60\,434.70 \pm 0.05) \text{ Mc},$$

or slightly lower than the value $(60\,435 \pm 1) \text{ Mc}$ of other observers.

IV. DISCUSSION

This investigation was carried to the point where satisfactory experimental verification of the gross features of the oxygen microwave absorption applicable to an atomic frequency standard was achieved. This

TABLE IV. Calculated frequency precision attainable by use of various improved operating conditions.

Quantity	Units	Reasonable conditions for present state of the art, in order of increasing experimental difficulty			Near-optimum conditions
		Bolometer	Bolometer	Superheterodyne	Superheterodyne
Type detector					
T	°K	300	76	76	45
$\Delta\nu$	Mc	0.330	0.175	0.175	0.130
P_0	mw	5	5	5	83
p	μ Hg	171	28.1	28.1	13.4
Transition		$N_+ = 9$	$N_- = 3$	$N_- = 3$	$N_- = 3$
ν_0	Mc	61 152	62 486	62 486	62 486
Wave-guide size	Wave-guide size	Wave-guide size	Wave-guide size	Wave-guide size	Wave-guide size
	cm×cm	0.356×0.711	0.356×0.711	0.356×0.711	0.432×1.067
α	10^{-6} cm $^{-1}$	1510	710	710	382
γ_0	10^{-6} cm $^{-1}$	22.6	212	212	506
$l = l_{opt}$	cm	653	1150	2300	3360
d		$1/\sqrt{3}$	$1/\sqrt{3}$	$1/\sqrt{3}$	$1/\sqrt{3}$
G	times	0.015	0.016	0.1	0.1
F	times	940	860	88	88
B	cps	1	1	1	1
$\delta\nu_n/\nu$		58×10^{-12}	1.8×10^{-12}	0.45×10^{-12}	2×10^{-14}

agreement was such as to allow confidence in extrapolation of these gross features to improved experimental conditions, but no attention has yet been paid to a number of effects small at the present level of accuracy, but which may emerge as limiting factors in accuracy as precision is further improved.

Because of the asymmetrical (VV-W) shape factor, containing $\Delta\nu$, the average of two frequencies on the steepest slope of the absorption line which undergo the same absorption is¹

$$\nu = \nu_0 [1 + (1/2)(\Delta\nu/\nu_0)^2]. \quad (24)$$

This effect will become important at the 10^{-10} level of accuracy for line widths of 0.85 Mc, and will vary with both pressure and temperature. This apparent shift should be amenable to treatment as a fairly well-known correction by recourse to the VV-W shape factor, and should not give trouble as an uncontrollable error until precision levels of 10^{-12} or so.

There may be a possible shift of ν_0 with pressure, analogous to the one for ammonia discussed by Margenau¹⁴ and Birnbaum and Maryott.¹⁵ This shift is below the level of detection at present, but may well appear at higher orders of precision.

Similarly, the influence of the tails of neighboring lines, contribution from isotopic lines, broadening by residual magnetic fields, and similar effects may all be expected to contribute error at some (high) level of

precision, and would have to be investigated as the appropriate precision level was reached experimentally.

It has been shown here that the product of line width and noise/signal ratio (which essentially determines $\delta\nu_n/\nu_0$) can be made very small for oxygen. In addition, the small dipole moment leading to low intermolecular forces and hence long state lifetimes and narrow lines, and the absence of any further magnetic dipole or electric quadrupole hyperfine structure in the transitions of $O^{16}O^{16}$ confirm its merit in a gas absorption type frequency standard. The large line width compared to beams and masers which enters into this product may produce greater vulnerability to systematic errors such as: (a) errors arising from insufficient knowledge of the shape of an asymmetric line; and (b) "pulling effects," or line shape distortion by other frequency-sensitive responses in the system. The latter point, however, is not extremely serious, for no severe frequency sensitivity appears in a matched absorption cell. Apart from these remarks, the disadvantage of a wide line of well-known shape in a given product of line width and noise/signal ratio probably is largely a psychological one.

ACKNOWLEDGMENT

The author is indebted to Dr. Harold Lyons for initiating and making possible the work on this problem, to Mr. George E. Schafer for collaboration in the early stages, to Mr. L. W. Miller, Jr. for assistance with the measurements, and to Mr. Ramon C. Baird for checking the calculations.

¹⁴ H. Margenau, Phys. Rev. 76, 1423 (1949).

¹⁵ G. Birnbaum and A. A. Maryott, Phys. Rev. 92, 270 (1953); A. A. Maryott and G. Birnbaum, Phys. Rev. 99, 1886 (1955).